

# Yrast spectroscopy of $N=82,83$ isotopes $^{136}\text{Xe}$ and $^{137}\text{Xe}$ from $^{248}\text{Cm}$ fission

P. J. Daly, P. Bhattacharyya, C. T. Zhang, and Z. W. Grabowski  
*Chemistry Department, Purdue University, West Lafayette, Indiana 47907*

R. Broda and B. Fornal  
*Chemistry Department, Purdue University, W. Lafayette, Indiana 47907*  
*and Niewodniczanski Institute of Nuclear Physics, PL-31342 Cracow, Poland*

I. Ahmad, T. Lauritsen, and L. R. Morss  
*Physics and Chemistry Divisions, Argonne National Laboratory, Argonne, Illinois 60439*

W. Urban  
*Institute of Experimental Physics, Warsaw University, PL-00681 Warsaw, Poland*

W. R. Phillips, J. L. Durell, M. J. Leddy, A. G. Smith, and B. J. Varley  
*Departments of Physics and Astronomy, University of Manchester, M13 9PL Manchester, United Kingdom*

N. Schulz, E. Lubkiewicz, and M. Bentaleb  
*Institut de Recherches Subatomiques, Université Louis Pasteur, F-67037 Strasbourg, France*

J. Blomqvist  
*Department of Physics Frescati, Royal Institute of Technology, S-10405 Stockholm, Sweden*  
 (Received 21 December 1998)

Prompt  $\gamma$ -ray cascades in neutron-rich nuclei around doubly magic  $^{132}\text{Sn}$  have been studied at Eurogam II using a  $^{248}\text{Cm}$  fission source. Here we report results for the four-valence-proton  $N=82$  nucleus  $^{136}\text{Xe}$  and for its  $N=83$  neighbor  $^{137}\text{Xe}$ . For both nuclei, the yrast level spectra have been considerably extended, and empirical nucleon-nucleon interactions have been used to assign probable shell model configurations. The  $^{136}\text{Xe}$  level energies are compared with those calculated using different sets of proton-proton interaction matrix elements, both diagonal and nondiagonal, obtained by fitting experimental data for other  $N=82$  isotones. [S0556-2813(99)00606-8]

PACS number(s): 23.20.Lv, 21.60.Cs, 25.85.Ca, 27.60.+j

## I. INTRODUCTION

There is special interest in the spectroscopy of the few-valence-particle nuclei around doubly magic  $^{132}\text{Sn}$ , which can yield information about nucleon-nucleon interactions and effective charges in an important sector of the nuclidic chart. Our knowledge of the structure of  $^{132}\text{Sn}$  and its neighbors derives mainly from  $\beta^-$  decay studies of short-lived fission product radionuclides, supplemented in a few cases by  $\gamma$ -ray decay data for yrast isomers. However, recent investigations using large  $\gamma$ -ray detector arrays to study fission fragments from actinide sources have identified prompt and delayed  $\gamma$ -ray cascades from individual product nuclei around  $^{132}\text{Sn}$ , and have opened prospects for broad and detailed exploration of the yrast spectroscopy of the region.

We have been investigating the yrast excitations in the  $Z=50-54$ ,  $N=80-84$  range of nuclei by analyzing fission product  $\gamma$ -ray data acquired at Eurogam II using a  $^{248}\text{Cm}$  source. First results for the two- and three-proton  $N=82$  isotones  $^{134}\text{Te}$  and  $^{135}\text{I}$  [1], for the  $N=83$  isotones  $^{134}\text{Sb}$ ,  $^{135}\text{Te}$ , and  $^{136}\text{I}$  [2], and for the two-neutron  $N=84$  nucleus  $^{134}\text{Sn}$  [3] have already been reported. For the  $N=82$  nuclei, empirical two-body interactions from the experimental  $\pi g_{7/2}^2$ ,  $\pi g_{7/2}d_{5/2}$ , and  $\pi g_{7/2}h_{11/2}$  multiplets in  $^{134}\text{Te}$  were used in

shell model calculations to characterize the corresponding three-proton states in  $^{135}\text{I}$ . Additionally, the highest-energy levels located in both  $^{134}\text{Te}$  and  $^{135}\text{I}$  were shown to be core-excited states involving  $\nu f_{7/2}h_{11/2}^{-1}$  particle-hole excitations. In a separate theoretical development, calculations by Andreozzi *et al.* [4] using an effective interaction derived from the Bonn A free nucleon-nucleon interaction gave excellent agreement with the experimental energies of the two- and three-proton states in  $^{134}\text{Te}$  and  $^{135}\text{I}$ .

We have now extended these studies to the four-valence-proton  $N=82$  nucleus  $^{136}\text{Xe}$  and to its  $N=83$  neighbor  $^{137}\text{Xe}$ . The investigation of  $^{136}\text{Xe}$  faced initial difficulties, since its predicted  $^{248}\text{Cm}$  fission yield is only 0.4% [5], smaller than the  $^{134}\text{Te}$  yield by a factor of 7; moreover, the yrast  $6^+$  state in  $^{136}\text{Xe}$  has a 3  $\mu\text{s}$  half-life, which ruled out the possibility of identifying higher-lying  $\gamma$  rays through prompt coincidences with known  $^{136}\text{Xe}$   $\gamma$  rays deexciting the isomer. However, close inspection of the  $\gamma\gamma$  cross coincidences observed with known  $^{106-109}\text{Mo}$   $\gamma$  rays led to firm identification of two moderately strong  $\gamma$ -ray cascades feeding the  $^{136}\text{Xe}$  3  $\mu\text{s}$  isomer, thus locating new high-lying yrast states in this nucleus. It was easier to study the  $N=83$  nucleus  $^{137}\text{Xe}$  because its  $^{248}\text{Cm}$  fission yield is higher (1.5%), and the only known yrast isomer in  $^{137}\text{Xe}$ , with a

half-life of  $\sim 8$  ns, in no way hindered the detection by  $\gamma\gamma$  coincidence measurements of  $\gamma$ -ray cascades feeding from above.

## II. EXPERIMENTAL PROCEDURE AND RESULTS

### A. Experimental

The  $\gamma$ -ray measurements were performed at the Eurogam II array using a  $^{248}\text{Cm}$  source which delivered  $\sim 6 \times 10^4$  fissions/sec. The fission fragments were stopped inside the source within about 2 ps, with subsequent emission of almost all the deexcitation  $\gamma$  rays from nuclei at rest. Eurogam II at the time consisted of 52 large Ge detectors in anti-Compton shields, including 24 four-crystal clover detectors which could serve as Compton polarimeters. In addition, four Low Energy Photon Spectrometer (LEPS) detectors were used to measure x rays and low-energy  $\gamma$  rays. In total, about  $2.5 \times 10^9$  threefold or higher-fold  $\gamma$ -ray coincidence events were recorded. These data were sorted into several  $\gamma\gamma\gamma$  cubic arrays and into two-dimensional  $\gamma\gamma$  matrices with both axes extending above 4 MeV.

A more complete account of the experimental details and of the data analysis has been given in earlier publications [1,6,7]. In particular, Urban *et al.* [6,7] have described how information about transition multipolarities could be extracted from analyses of double and triple  $\gamma$ -ray angular correlations and from directional-polarization correlations of  $\gamma$  rays. In the present work, these techniques were used to characterize a number of the strongest transitions in  $^{137}\text{Xe}$ , but the  $^{136}\text{Xe}$   $\gamma$  rays of interest were all too weak.

### B. Extending the $^{136}\text{Xe}$ level scheme

A  $2.95 \mu\text{s}$   $6^+$  isomer at 1892 keV in  $^{136}\text{Xe}$  is well established from studies of the  $^{136}\text{I} \pi^-(6^-)$   $\beta$  decay [8], and of delayed  $\gamma$  rays following  $^{252}\text{Cf}$  fission [9,10]. The isomer deexcites by a cascade of 197, 381, and 1313 keV  $E2$  transitions to the  $^{136}\text{Xe}$  ground state. A second  $6^+$  state at 2262 keV, also fed in the  $^{136}\text{I}$   $\beta$  decay, deexcites exclusively to the  $3 \mu\text{s}$  isomer by a 370 keV  $M1/E2$  transition. Up to now, no states with  $I > 6$  have been placed in the  $^{136}\text{Xe}$  scheme.

In the present work, possible  $\gamma$ -ray cascades populating the long-lived  $^{136}\text{Xe}$   $6^+$  isomer following  $^{248}\text{Cm}$  fission could not be identified from the available  $\gamma\gamma\gamma$  coincidence data in any straightforward way. For example, a double gate on the 381 and 1313 keV  $\gamma$  rays deexciting the lowest  $4^+$  state in  $^{136}\text{Xe}$  showed in coincidence [Fig. 1(a)] a few strong  $^{136}\text{Xe}$   $\gamma$  rays, all known transitions feeding the  $4^+$  state directly, as well as cross-coincident  $^{106-109}\text{Mo}$   $\gamma$  rays from complementary fission fragments. In fact, the strongest peaks in Fig. 1(a) are the 193, 371, and 527 keV  $\gamma$  rays of  $^{108}\text{Mo}$ , which is the fission partner of  $^{136}\text{Xe}$  in the case of  $4n$  emission. Double gating on the 371 and 527 keV  $\gamma$  rays showed in coincidence [Fig. 1(b)] known  $\gamma$  rays of  $^{108}\text{Mo}$ ,  $^{136}\text{Xe}$ ,  $^{137}\text{Xe}$ , and  $^{138}\text{Xe}$ , as well as other lines that could not immediately be assigned with confidence. Of these, the 370 keV  $\gamma$  ray in Fig. 1(b) was likely to be the  $^{136}\text{Xe}$   $6_2^+ \rightarrow 6_1^+$  transition previously mentioned, while the prominent 968 and 975 keV  $\gamma$  rays also appeared attractive candidates for placement in  $^{136}\text{Xe}$  above the  $3 \mu\text{s}$  isomer. The 370 and 968 keV  $\gamma$  rays were subsequently found to be in prompt coin-

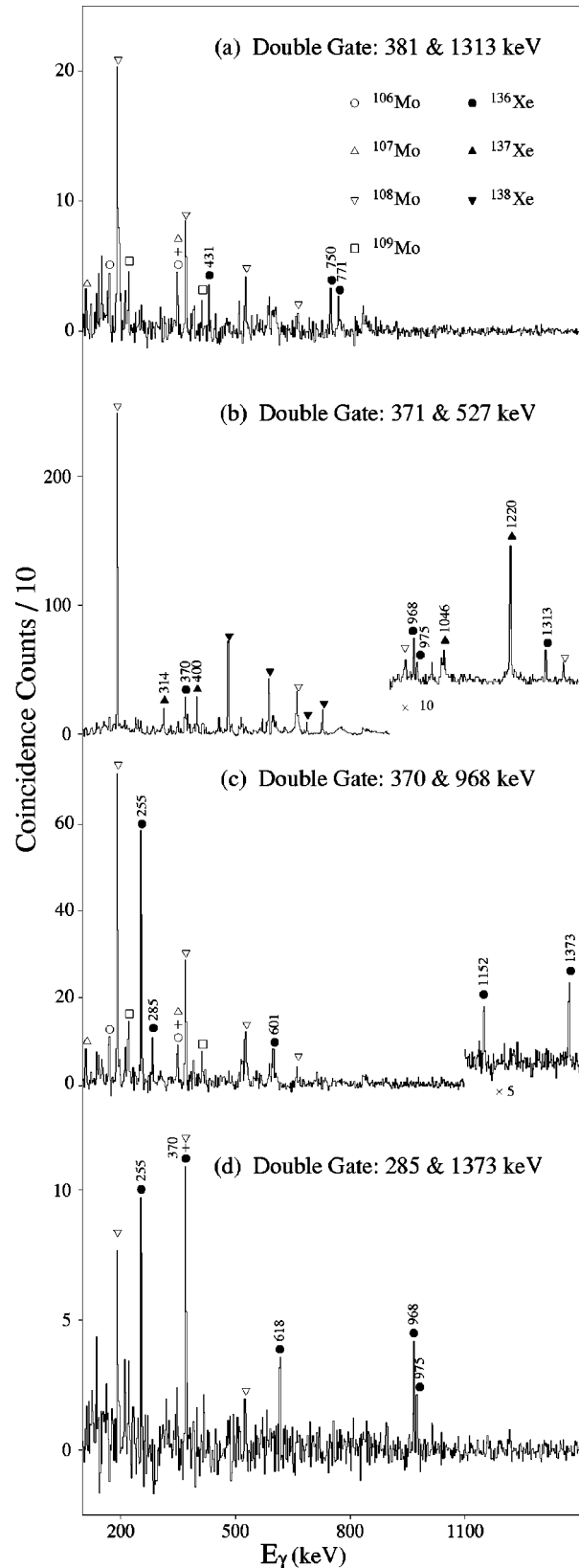


FIG. 1. Key  $\gamma\gamma$  coincidence spectra for isotopic identification of  $^{136}\text{Xe}$  transitions and construction of the  $^{136}\text{Xe}$  level scheme.

cence, but not the 370 and 975 keV  $\gamma$  rays. Double gating on the 370 and 968 keV  $\gamma$  rays generated the coincidence spectrum of Fig. 1(c), where the relative intensities of the cross-coincident  $^{106,107,108,109}\text{Mo}$   $\gamma$  rays are seen to be

TABLE I. Energies and relative intensities of  $^{136}\text{Xe}$   $\gamma$  rays above the 3  $\mu\text{s}$  isomer observed following  $^{248}\text{Cm}$  fission. Except for the weakest lines, the energy error is estimated to be about 0.3 keV and the intensity error to be less than 20%.

$E_\gamma$ (keV)	Relative $\gamma$ -ray intensity	Placement $E_i \rightarrow E_f$ (keV)
221.0	3	6173 $\rightarrow$ 5953
255.0	40	3484 $\rightarrow$ 3229
284.5	11	5143 $\rightarrow$ 4858
369.8	100	2262 $\rightarrow$ 1892
600.8	11	3830 $\rightarrow$ 3229
617.8	25	3484 $\rightarrow$ 2867
967.8	67	3229 $\rightarrow$ 2262
975.1	75	2867 $\rightarrow$ 1892
1094.3	5	5953 $\rightarrow$ 4858
1151.6	6	4381 $\rightarrow$ 3229
1373.2	14	4858 $\rightarrow$ 3484
1657.8	4	5143 $\rightarrow$ 3484

closely similar to those in Fig. 1(a), thus providing vital support for the assignments of the 370 and 968 keV  $\gamma$  ray pair to  $^{136}\text{Xe}$ . Finally a double gate on 285 and 1373 keV  $\gamma$  rays, two high-lying transitions in  $^{136}\text{Xe}$ , exhibits [Fig. 1(d)] the two main cascades feeding the  $6^+$  isomer, one consisting of the 255, 968, and 370 keV transitions, the other in parallel with the 618 and 975 keV transitions. The extended  $^{136}\text{Xe}$  level scheme is displayed in Fig. 3, below, where tentative spin-parity assignments and dominant four-proton configurations are also indicated. These assignments are discussed below, and the relative intensities of  $^{136}\text{Xe}$  transitions above the 3  $\mu\text{s}$  isomer are shown in Table I.

### C. Extending the $^{137}\text{Xe}$ scheme

Many years ago, a study of delayed  $\gamma$  rays following  $^{252}\text{Cf}$  fission [10] identified and assigned to the  $N=83$  nucleus  $^{137}\text{Xe}$  a cascade of 314, 400, and 1221 keV  $\gamma$  rays deexciting an isomer with  $t_{1/2} \sim 8$  ns. The same  $\gamma$  rays had previously been reported in Ref. [9], where they were not assigned. The levels of  $^{137}\text{Xe}$  populated in  $^{137}\text{I}$   $\beta$  decay include a 1220 keV level with  $I^\pi = 11/2^-$  that deexcites to the  $7/2^-$  ground state with emission of a 1220.1 keV  $\gamma$  ray [11,12]; this transition and the one observed in the 8 ns isomeric decay are probably identical. Indeed, a first inspection of the data from the present  $^{248}\text{Cm}$  fission product measurements revealed intense 314.0, 400.2, and 1220.0 keV  $\gamma$  rays in mutual coincidence. This strong three- $\gamma$ -ray cascade provided an excellent starting point for further investigation of the  $^{137}\text{Xe}$  yrast level structure.

Some important  $\gamma$ -ray coincidence spectra for  $^{137}\text{Xe}$  are displayed in Fig. 2. Detailed analyses of these and the rest of the  $\gamma\gamma\gamma$  data established the  $^{137}\text{Xe}$  level scheme shown in Fig. 3, which accommodates almost all the observed  $\gamma$  rays. Omitted from this simplified scheme are four near-yrast levels of  $^{137}\text{Xe}$  at 1978, 2103, 3112, and 3252 keV, which are only weakly populated following  $^{248}\text{Cm}$  fission. All the  $\gamma$  rays assigned here to  $^{137}\text{Xe}$  are listed in Table II, where their placements are also indicated. For the stronger  $^{137}\text{Xe}$  transitions, the angular correlation data provided useful multipo-

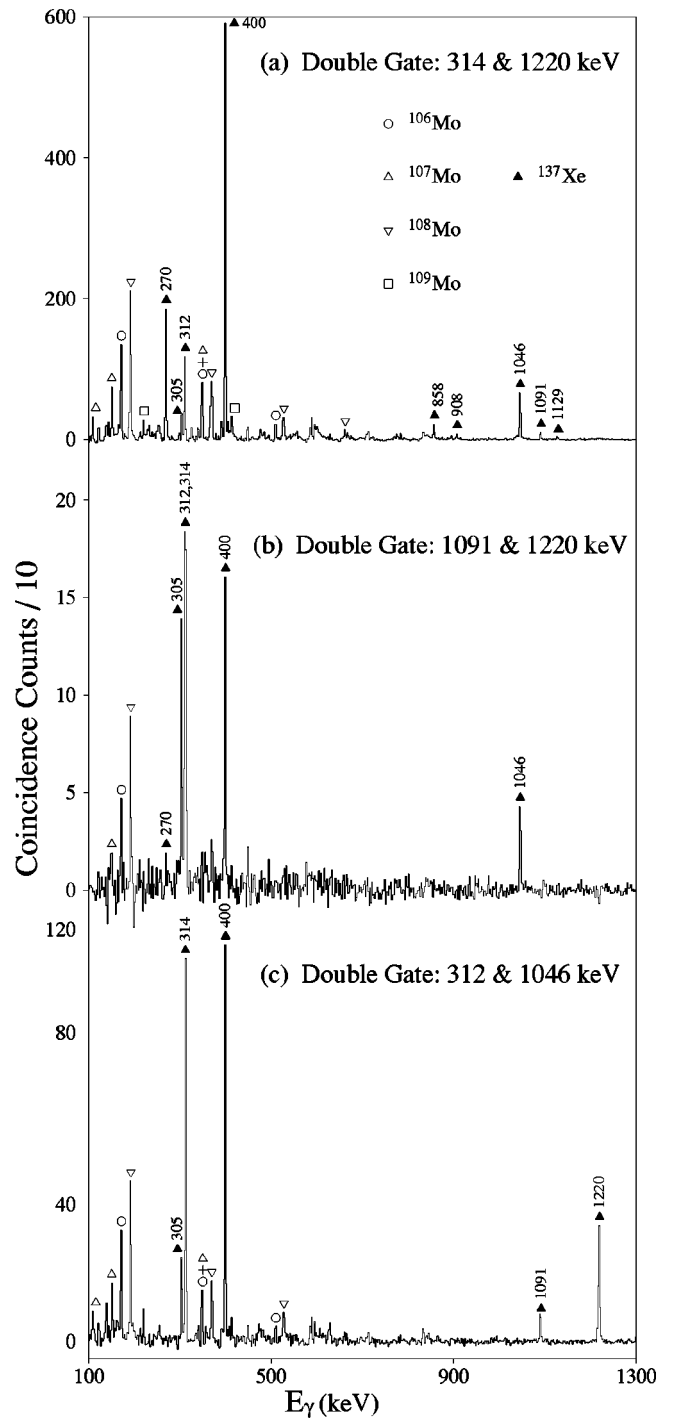


FIG. 2. Key  $\gamma\gamma$  coincidence spectra for  $^{137}\text{Xe}$ .

larity information, as summarized in Table III. Thus the 314 and 400 keV  $\gamma$  rays following the  $\sim 8$  ns isomer could be characterized as stretched quadrupoles, and the linear polarization results showed that they both have  $E2$  character, establishing at  $I^\pi = 19/2^-$  for the isomeric state. The polarization measurements indicated stretched  $E2$  character also for the 312 keV transition, but they were inconclusive for the other transitions. Special mention is made of the strong 270 keV transition feeding the  $19/2^-$  isomeric state which is interpreted as a  $\Delta I=0$   $M1/E2$  transition analogous to the strong 370 keV  $6_2^+ \rightarrow 6_1^+$   $M1/E2$  transition in  $^{136}\text{Xe}$ .

The spin-parity assignments proposed for the  $^{137}\text{Xe}$  levels in Fig. 3 are consistent with all the experimental results.

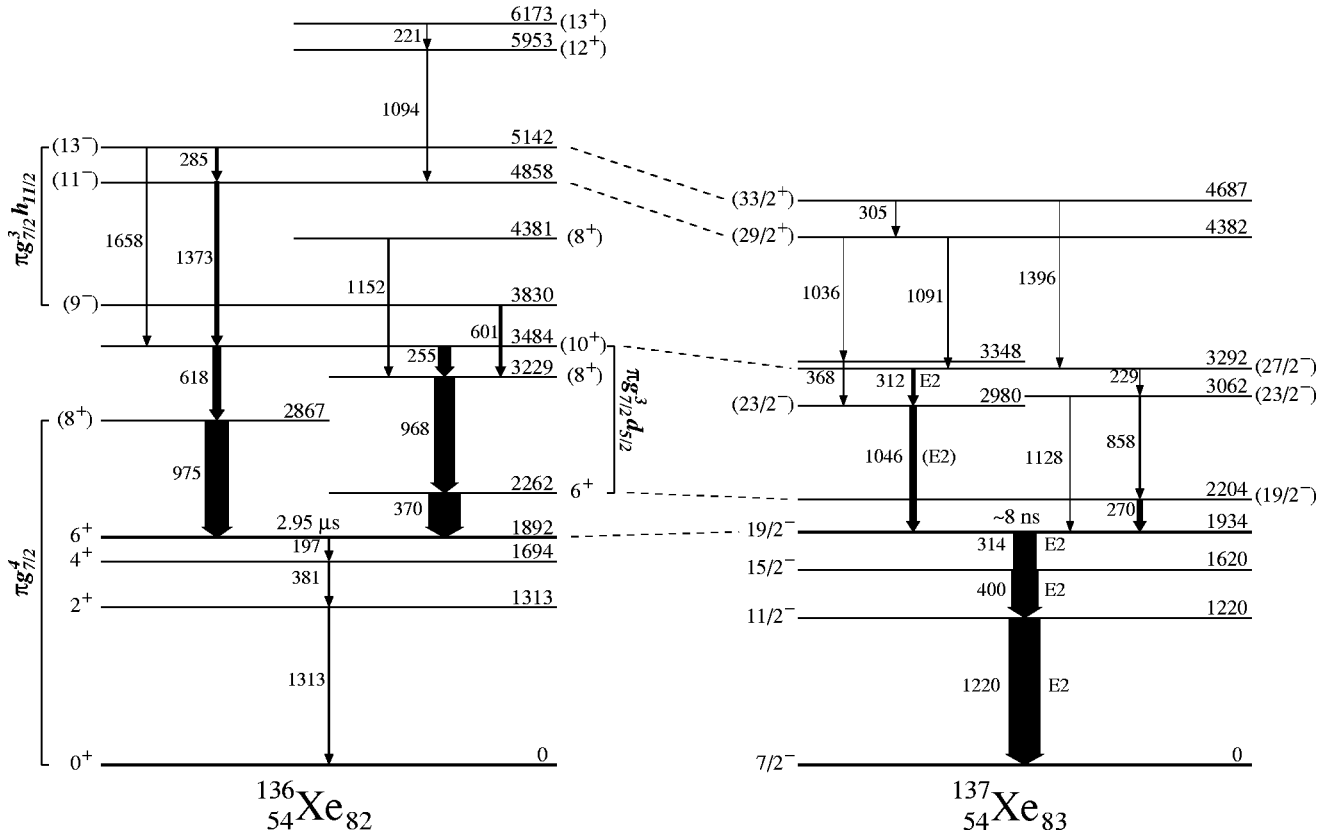


FIG. 3. The  $^{136}\text{Xe}$  and  $^{137}\text{Xe}$  level schemes with dominant shell model configurations indicated.

TABLE II. Energies and relative intensities of  $^{137}\text{Xe}$   $\gamma$  rays observed following  $^{248}\text{Cm}$  fission. Except for the weakest lines, the energy error is estimated to be about 0.3 keV and the intensity error to be less than 20%.

$E_\gamma$ (keV)	Relative $\gamma$ ray intensity	Placement $E_i \rightarrow E_f$ (keV)
101.1	<1	2204 $\rightarrow$ 2103
124.9	$\sim 1$	2103 $\rightarrow$ 1978
139.5	$\sim 1$	3252 $\rightarrow$ 3112
190.2	$\sim 1$	3252 $\rightarrow$ 3062
229.4	$\sim 1$	3292 $\rightarrow$ 3062
269.7	19	2204 $\rightarrow$ 1934
304.8	3	4687 $\rightarrow$ 4382
311.6	12	3292 $\rightarrow$ 2980
314.0	63	1934 $\rightarrow$ 1620
358.2	8	1978 $\rightarrow$ 1620
367.7	3	3348 $\rightarrow$ 2980
400.2	87	1620 $\rightarrow$ 1220
483.3	6	2103 $\rightarrow$ 1620
857.9	5	3062 $\rightarrow$ 2204
907.4	2	3112 $\rightarrow$ 2204
1035.6	1	4382 $\rightarrow$ 3348
1045.8	21	2980 $\rightarrow$ 1934
1090.8	3	4382 $\rightarrow$ 3292
1128.3	2	3062 $\rightarrow$ 1934
1220.0	100	1220 $\rightarrow$ 0
1396.0	1	4687 $\rightarrow$ 3292

Broad correspondence between the  $^{136}\text{Xe}$  and  $^{137}\text{Xe}$  yrast excitations is evident, with most prominent features of the  $^{137}\text{Xe}$  level structure attributable to the coupling with an additional  $f_{7/2}$  valence neutron.

### III. DISCUSSION

One of the main objectives in studying the spectroscopy of few-valence-particle nuclei around  $^{132}\text{Sn}$  is to characterize the nucleon-nucleon interactions in this region. To perform shell model calculations for the  $N=82$  isotones, the simplest method is to adopt two-body interactions from the experi-

TABLE III. Angular correlation results and multipolarity assignments for  $^{137}\text{Xe}$  transitions. In all cases, the gating  $\gamma$  ray is the 1220 keV stretched  $E2$  transition.

$E_\gamma$ (keV)	$W(\theta)$				Assignment
	$0^\circ$	$30^\circ$	$60^\circ$	$90^\circ$	
400	1.14(2)	1.09(1)	1.01(1)	1.00(1)	$\Delta I=2, E2$
314	1.19(2)	1.11(1)	1.03(1)	1.00(1)	$\Delta I=2, E2$
1046	1.20(3)	1.08(1)	1.03(1)	1.00(1)	$\Delta I=2$
270	1.24(2)	1.17(1)	1.07(1)	1.00(1)	$\Delta I=0$ , see text
1128	1.35(31)	1.11(7)	1.01(5)	1.00(7)	( $\Delta I=2$ )
312	1.18(2)	1.12(1)	1.05(1)	1.00(1)	$\Delta I=2, E2$
368	0.86(5)	0.92(2)	0.95(2)	1.00(2)	$\Delta I=1$
1091	0.89(10)	0.91(4)	0.97(2)	1.00(4)	$\Delta I=1$
1396	1.3(5)	1.43(12)	1.16(10)	1.00(15)	( $\Delta I=2$ )

TABLE IV. The experimental level energies in  $^{136}\text{Xe}$  are compared with theoretical energies calculated using diagonal matrix elements from  $^{134}\text{Te}$  (DIAG), and using the best fit parameter sets of Wildenthal (WILD) and Blomqvist (BLOM) discussed in the text.

$I^\pi$	Expt. (keV)	DIAG (keV)	WILD (keV)	BLOM (keV)
$0^+$	0	0	0	15
$2^+$	1313	1279	1314	1372
$4^+$	1694	1577	1714	1717
$6^+$	1892	1691	1846	1858
$6^+$	2262	2097	2260	2236
$8^+$	2867	2666	2931	2862
$8^+$	3229	3200	3230	3242
$10^+$	3484	3499	3582	3484
$(9^-)$	3830	3666	3738	3840
$(11^-)$	4858	4783	4844	4923
$(13^-)$	5142	5047	5157	5138

mental level spectrum of the two-proton nucleus  $^{134}\text{Te}$ . This approach, which takes account of diagonal matrix elements only, and thereby neglects configuration mixing, provided valuable guidance in the initial interpretation of the observed  $^{136}\text{Xe}$  levels, which were thus assigned the dominant four-proton configurations indicated in Fig. 3. The experimental  $^{136}\text{Xe}$  level energies may be compared in Table IV with the values calculated using diagonal matrix elements taken from the  $^{134}\text{Te}$  spectrum. The agreement is seen to be only fair, but this is in line with expectations of appreciable mixing between such configurations as  $\pi g_{7/2}^4$ ,  $\pi g_{7/2}^3 d_{5/2}$ , and  $\pi g_{7/2}^2 d_{5/2}^2$ . Lawson [13] and others have already noted that the yrast  $6^+ \rightarrow 4^+$  transition in  $^{136}\text{Xe}$  is unusually slow [ $B(E2) < 0.02$  Weisskopf units (W.u.)], a clear indication that the  $\pi g_{7/2}$  subshell is very close to being half-filled in these states.

A few years ago, Wildenthal [14] carried out a detailed analysis of the level spectra of  $N=82$  isotones ranging from  $^{133}\text{Sb}$  to  $^{154}\text{Hf}$ . In a model space consisting of the  $g_{7/2}$ ,  $d_{5/2}$ ,  $d_{3/2}$ ,  $s_{1/2}$ , and  $h_{11/2}$  proton orbits, he performed, with some

truncation, comprehensive shell model calculations, and used an iterative procedure to extract a best-fit set of five single particle energies and 160 two-body matrix elements, both diagonal and off diagonal. These parameters were found to be consistent with the extensive body of spectroscopic observables then available for the  $N=82$  isotones [14]. When the  $^{136}\text{Xe}$  level energies were here recalculated using the Wildenthal parameter set, much better overall agreement with experiment was obtained (Table IV).

Since our results for  $^{135}\text{I}$  and  $^{136}\text{Xe}$  are significant additions to the data set, and all the required proton single particle energies are now known from experiment, Blomqvist has recently updated the  $N=82$  interaction parametrization and has changed 54 of Wildenthal's matrix elements, mostly diagonal ones. Details will be presented elsewhere [15]. As shown in Table IV, these changes improve the agreement between theory and experiment for  $^{136}\text{Xe}$ , if only to a small extent. The following paper [16] presents first results for the five valence proton nucleus  $^{137}\text{Cs}$ , which were still unknown when the input parameters for the  $N=82$  shell model calculations were modified. The new  $^{137}\text{Cs}$  data are thus particularly suitable for testing the updated set of nucleon-nucleon interaction matrix elements presented in Ref. [15].

The highest levels located at 5953 and 6173 keV in  $^{136}\text{Xe}$  are probably core-excited  $\pi g_{7/2}^4 \nu f_{7/2} h_{11/2}^{-1}$  states corresponding to the yrast  $12^+$  and  $13^+$  states at  $\sim 6$  MeV in  $^{134}\text{Te}$ . Moreover, the lower  $^{136}\text{Xe}$  level at 4381 keV may be the  $8^+$  core excitation built on the ground state, analogous to the known  $8^+$  states in  $^{132}\text{Sn}$  and  $^{134}\text{Te}$  at 4848 and 4557 keV, respectively. The  $8^+$  energy systematics supports this interpretation.

#### ACKNOWLEDGMENTS

This work was supported by the U.S. Department of Energy under Contracts Nos. DE-FG02-87ER40346 and W-31-109-ENG-38, by the Science and Engineering Council under Grant No. GRH 71161, and by Polish Scientific Committee Grant No. 2PO3B-150-10. The authors are indebted for the use of  $^{248}\text{Cm}$  to the Office of Basic Energy Sciences, U.S. Department of Energy, through the transplutonium element production facilities at the Oak Ridge National Laboratory.

- [1] C. T. Zhang *et al.*, Phys. Rev. Lett. **77**, 3743 (1996).  
 [2] P. Bhattacharyya *et al.*, Phys. Rev. C **56**, R2363 (1997).  
 [3] C. T. Zhang *et al.*, Z. Phys. A **358**, 9 (1997).  
 [4] F. Andreozzi *et al.*, Phys. Rev. C **56**, R16 (1997).  
 [5] A. C. Wahl, At. Data Nucl. Data Tables **39**, 1 (1988).  
 [6] W. Urban *et al.*, Nucl. Instrum. Methods Phys. Res. A **365**, 596 (1995).  
 [7] W. Urban *et al.*, Z. Phys. A **358**, 145 (1997).  
 [8] P. F. Mantica *et al.*, Phys. Rev. C **43**, 1696 (1991).  
 [9] W. John, F. W. Guy, and J. J. Weselowski, Phys. Rev. C **2**, 1451 (1970).  
 [10] R. G. Clark, L. E. Glendenin, and W. L. Talbert, in Proceedings of the *Third IAEA Symposium on the Physics and Chemistry of Fission*, Rochester, 1973 (International Atomic Energy Agency, Vienna, 1974), Vol. 2, p. 221.  
 [11] B. Fogelberg and H. Tovedal, Nucl. Phys. **A345**, 13 (1980).  
 [12] P. Hoff, B. Ekström, and B. Fogelberg, Z. Phys. A **332**, 407 (1989).  
 [13] R. D. Lawson, *Theory of the Nuclear Shell Model* (Clarendon, Oxford, 1980), p. 325.  
 [14] B. H. Wildenthal, in *Understanding the Variety of Nuclear Excitations*, edited by A. Covello (World Scientific, Singapore, 1991).  
 [15] J. Blomqvist, in Proceedings of the XXXIII Zakopane School of Physics, 1998, edited by R. Broda, B. Fornal, and W. Meczynski [Acta Phys. Pol. B (to be published)].  
 [16] R. Broda *et al.*, Phys. Rev. C **59**, 3071 (1999), the following paper.